18TH WORLD CONFERENCE ON EARTHQUAKE ENGINEERING
WCEE2024
MILAN

MILAN, ITALY
30TH JUNE - 5TH JULY 2024
www.wcee2024.it

SIMULATION OF LATERAL BEHAVIOUR OF UN-STRENGTHENED AND FERROCEMENT STRENGTHENED MASONRY INFILLED RC FRAME

D. Sen[1], M. Hassan[2], A. Dutu[3], M. Seki[4] & M. Maeda[5]

[1] Ahsanullah University of Science and Technology, Dhaka, Bangladesh, dsendip@gmail.com

[2] Housing and Building Research Institute, Dhaka, Bangladesh

[3] Technical University of Civil Engineering Bucharest, Bucharest, Romania

[4] Building Research Institute, Tsukuba, Japan

[5] Tohoku University, Sendai, Japan

Abstract: *In developing countries like Bangladesh, several masonry-infilled RC buildings are under severe threat because of inadequacies in seismic design. Damages of such buildings in recent earthquakes, e.g., the Turkey-Syria Earthquake 2023, demonstrate the necessity of seismic evaluation and strengthening of existing masonry-infilled RC buildings. To mitigate strength inadequacy, ferrocement (FC) strengthening can be utilized to improve the lateral capacity of masonry-infilled RC buildings. The seismic assessment of such un-strengthened and ferrocement strengthened masonry-infilled RC buildings can be conducted by non-linear static analysis. Non-linear static analysis can predict the overall lateral behaviour of a building as well as the damage extent of structural members under seismic events. Numerical modelling and non-linear analysis of RC frame, masonry infilled RC frame, and ferrocement strengthened masonry infilled RC frame can be conducted in SAP2000. The nonlinearity of structural elements can be considered using lumped plasticity models in SAP2000. Therefore, it is necessary to verify the performance of the above-mentioned numerical models to predict overall lateral behaviour against experimental lateral behaviour.*

In this study, the lateral behaviour of one single-story single-bay bare RC frame, one masonry-infilled RC frame, and one ferrocement strengthened masonry-infilled RC frame has been simulated by SAP2000 software using experimental data from the authors' previous study. The RC frame has been modelled considering lumped nonlinear hinges at the ends of the beam and column. The nonlinear hinge properties of RC elements have been adopted from FEMA 356 guidelines. Meanwhile, both un-strengthened and ferrocement strengthened masonry infills have been modelled as a single diagonal strut. The nonlinear behaviour of the axial hinge on the strut has been suggested and utilized. The numerical analysis result shows that the developed numerical models, i.e., bare RC frame, masonry infilled RC frame, and ferrocement strengthened masonry infilled RC frame, can predict the lateral behaviour fairly when compared with experimental lateral behaviour.

1. Introduction

Seismic evaluation and strengthening are some of the most crucial concerns for structural engineers in developing countries because there are so many seismically vulnerable buildings. Many of such vulnerable buildings are masonry infilled RC frames where infill masonry is considered a non-structural element, although it commonly affects the structural performance (Alwashali et al., 2020). In addition, damages of such masonry infilled buildings in recent earthquakes, e.g., the Turkey-Syria Earthquake 2023, demonstrate the necessity of strengthening existing vulnerable masonry-infilled RC buildings. To mitigate strength inadequacy, ferrocement (FC) strengthening can be utilized to improve the lateral capacity of masonry infilled RC buildings. Several researchers (Sen, 2020; Seki et al., 2018; Kaya et al., 2018; Demirel et al., 2015; Altin et al., 2010; Amanat et al., 2007 and Zarnic et al.,1985) found ferrocement as an effective scheme to improve the lateral capacities of masonry infilled RC frames. However, studies on numerical modelling of ferrocement strengthened masonry infilled RC frames are limited. In this context, an attempt has been made to model and analyse ferrocement strengthened masonry infilled RC frame, in addition to masonry infilled RC frame and bare RC frame, using the macro-modelling technique. Non-linear static analysis can predict the overall lateral behaviour of a building as well as the damage extent of structural members under seismic events. Numerical modelling and non-linear analysis of RC frame, masonry infilled RC frame, and ferrocement strengthened masonry infilled RC frame can be conducted in SAP2000 (CSI, 2014). The nonlinearity of structural elements can be considered using lumped plasticity models in SAP2000. Therefore, it is necessary to verify the performance of the above-mentioned numerical models to predict overall lateral behaviour against experimental lateral behaviour.

In this study, the lateral behaviour of one single-story single-bay bare RC frame, one masonry-infilled RC frame, and one ferrocement (FC) strengthened masonry-infilled RC frame has been simulated by SAP2000 software using experimental data from the author's previous study (Sen et al., 2020). The RC frame has been modelled considering lumped nonlinear hinges at the ends of the beam and column. The nonlinear hinge properties of RC elements have been adopted from FEMA 356 (2000). Meanwhile, both un-strengthened and ferrocement strengthened infill masonries have been modelled as a single diagonal strut. The nonlinear behaviour of the axial hinge on the strut has been suggested and utilized. The numerical analysis result shows that the developed numerical models, i.e., bare RC frame, masonry infilled RC frame, and ferrocement strengthened masonry infilled RC frame, can predict the lateral behaviour fairly when compared with experimental lateral behaviour.

2. Reference test specimens

2.1 Specimen details

The reference specimens have been taken from the authors' previous study. The experimental program consisted of three half-scaled specimens including a bare RC frame (S1-F), a masonry infilled RC frame (S3-FM), and a Ferro-cement strengthened masonry infilled RC frame (S5 FMFC). Details of all specimens are presented in Table 1 and Fig. 1 (a)-(c). Material properties of concrete and reinforcing steels used in the specimens are given in Table 2. The material properties of masonry and Ferro-cement coating are shown in Table 3. The wire mesh was tested as per ACI 549 (1997); however, the yield strength of the wire could not be identified by the material test. Therefore, the yield strength of wire mesh has been considered as $f_{y,wm}$ = 0.71$f_{u,wm}$ as per AS/NZS (2001), where $f_{y,wm}$, $f_{u,wm}$ = yield, and ultimate strength of wire mesh, respectively. All the specimens were subjected to cyclic lateral loading and a constant axial load of 350 kN on each column. More details can be found in Sen et al. (2020).

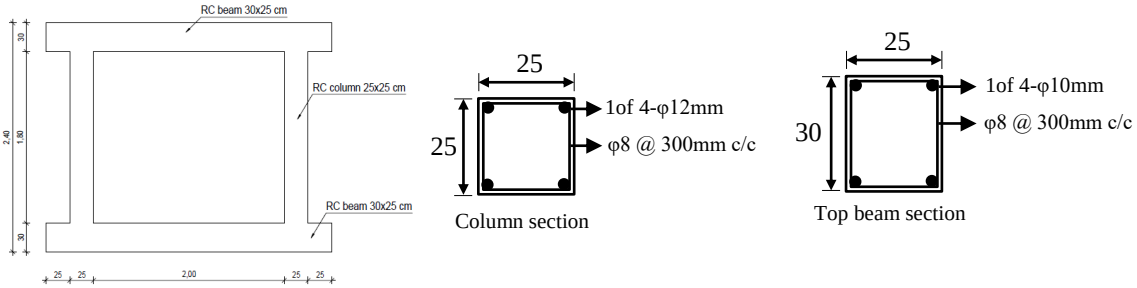

(a) Reinforced concrete (RC) frame (S1-F)

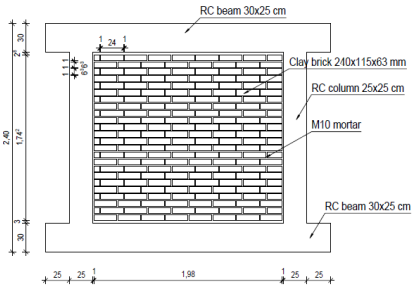

(b) Masonry infilled RC frame (S3-FM)

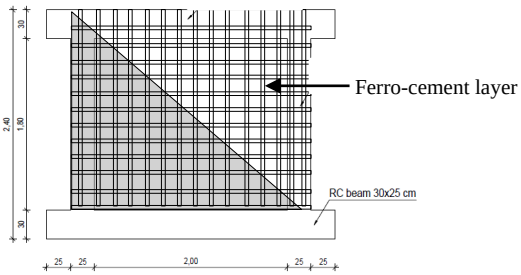

(c) Ferro-cement laminated masonry infilled RC frame (S5-FMFC)

Figure 1. Dimension and reinforcement detailing of test specimens (dimensions are in cm) (Sen et al., 2020)

Table: 1 Details of all specimens (Sen et al., 2020)

Specimen	***RC column***		***Masonry***	***Ferro-cement***			
	Dimension	**Main reinforcement**	**Thickness t_{mas}**	**Thickness t_{FC}**	**Wire diameter φ_{wm}**	**Wire spacing s**	**Number of mesh layers**
	mm		(mm)	(mm)	(mm)	(mm)	
S1-F			-	-	-	-	-
S3-FM	250 x 250	4-φ12mm	115	-	-	-	-
S5-FMFC			115	20	0.9	13	2

Table 2: Material Properties for concrete and steel (all values are in MPa) (Sen et al., 2020)

Specimen	**Concrete**	**Reinforcement**					
	$f_{c'}$	**Φ8**		**Φ10**		**Φ12**	
		f_y	f_{ult}	f_y	f_{ult}	f_y	f_{ult}
S1-F, S3-FM, S5-FMFC	14	364	429	454	553	428	525

$f_{c'}$= concrete compressive strength, f_y, f_{ult} = yield and ultimate strength of reinforcement

Table: 3 Material Properties for masonry and ferro-cement coating (all values are in MPa) (Sen et al., 2020)

Specimen	**Masonry**		**Ferro-cement**		
			Mortar	**Wire mesh**	
	f_{mas}	$f_{mor,j}$	$f_{mor,FC}$	$f_{u,wm}$	$f_{y,wm}$
S1-F	-	-	-	-	-
S3-FM	11.6	6.1	-	-	-
S5-FMFC	11.6	8.8	4.8	629	447

f_m= masonry compressive strength; $f_{mor,j}$, $f_{mor,FC}$ = mortar compressive strength of joint and Ferro-cement mortar; $f_{y,wm}$, $f_{u,wm}$ = yield and ultimate strength of wire mesh.

3. Modelling of specimens in SAP2000

The reference bare RC frame, masonry infilled RC frame and ferrocement strengthened masonry infilled RC frame have been modelled in SAP2000 v14. Details are discussed in the following subsections:

3.1 Bare RC frame

An idealized RC frame modelled in SAP2000 is shown in Fig. 2. The beam and column of the RC frame have been modelled as a line element. The concrete and reinforcing steel properties have been defined and assigned in column and beam according to the reference test frame properties as mentioned in Table 2. The cross-section of each element has been generated using the "Section Designer" feature of SAP2000. The generated cross sections are shown in Fig. 3. The columns have been fixed at the bottom. An axial load of 350 kN has been assigned as a dead load on the top of each column. The increasing lateral load has been applied using the displacement-controlled pushover feature of SAP2000. The nonlinearity of the beam and column have been assigned by using flexural hinges at both ends of each line element as shown in Fig. 2. The auto hinge properties of SAP2000 have been utilized for each beam and column. The auto hinge properties for concrete members have been adopted from FEMA 356 (2000). The default hinge properties "Auto M3" and "Auto P-M3" have been defined and assigned to the beam and column elements at a relative distance of 0.05 and 0.95 of the concerned members. The auto hinge assignment data of the beam and column are shown in Fig. 4(a) (b).

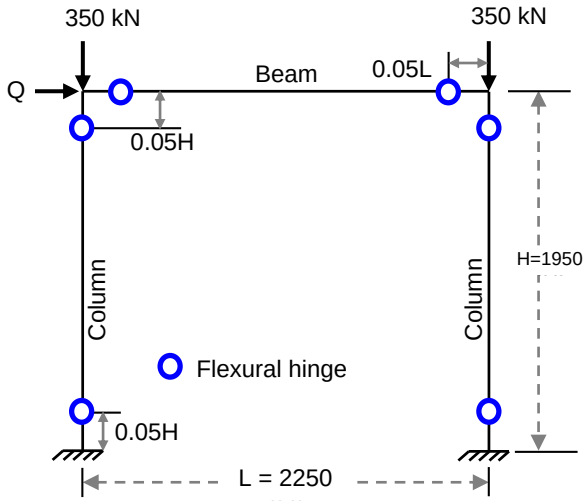

Figure 2. Idealized model of bare RC frame

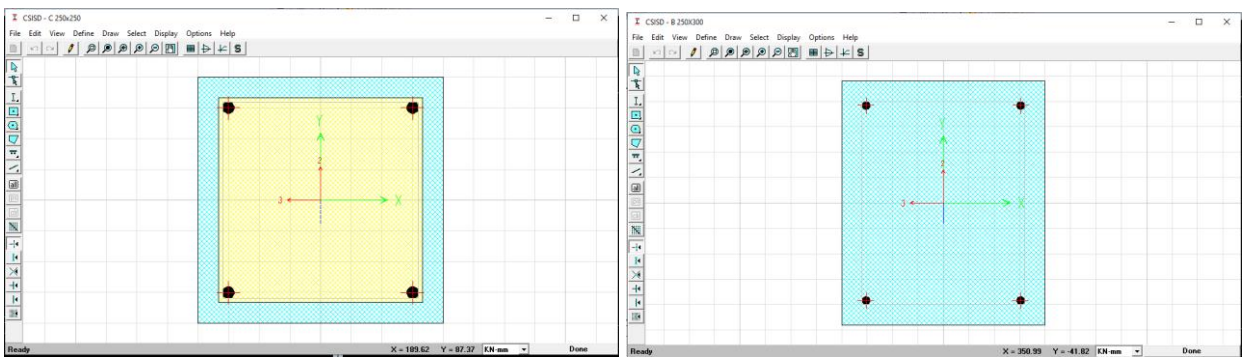

(a) *(b)*

Figure 3. Cross section of (a) column and (b) beam generated using Section Designer of SAP2000

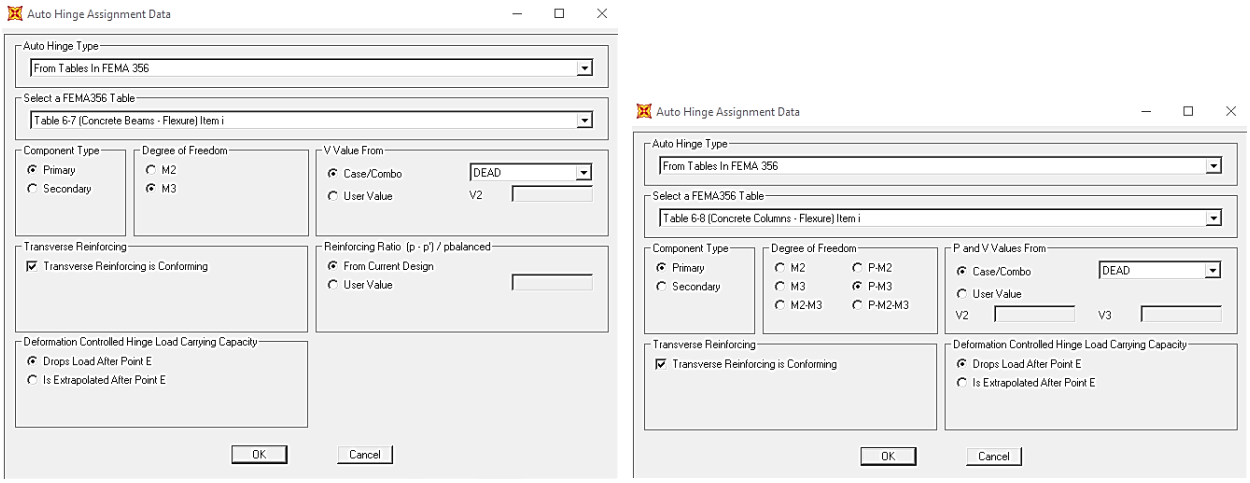

(a) *(b)*

Figure 4. Auto hinge assignment data of (a) beam and (b) column of the idealized model of bare RC frame

3.2 Masonry infilled RC frame

An idealized masonry infilled RC frame, modelled in SAP2000, is shown in Fig. 5(a). The idealized model consists of RC frame and an equivalent single masonry strut. The surrounding RC frame has been modelled in a similar way as discussed in the earlier sub-section. The equivalent strut has been modelled considering the masonry properties presented in Table 3, and a strut width that has been computed using Eq. (1) - (2) as per FEMA 273 (1997). The strut thickness has been considered as the thickness of the infill masonry.

$$W_s = 0.175(\lambda_1 h_{col})^{-0.4} d_m \quad (1)$$

$$\lambda_1 = \sqrt[4]{\frac{E_{mas} t_{mas} sin2\theta}{4 E_c I_c h_{mas}}} \quad (2)$$

where, W_s = masonry strut width; h_{col} = height of columns; d_m = diagonal length of masonry strut; E_{mas}/E_c = elastic modulus of masonry and concrete, respectively; I_c = moment of inertia of column; h_{mas} = height of masonry infill; t_{mas} = thickness of masonry, and θ = angle of masonry strut with horizontal.

An axial hinge, as shown in Fig. 5(a), has been assigned at the diagonal strut' mid-point to catch the nonlinear behaviour of masonry. The nonlinearity of the masonry strut has been considered as per Islam and Sen (2023) where the axial load-displacement behaviour of the equivalent strut has been suggested considering the sliding failure of infill masonry, as shown in Fig. 5(b). This particular model has been utilized since the experimental failure of the infill was a sliding failure.

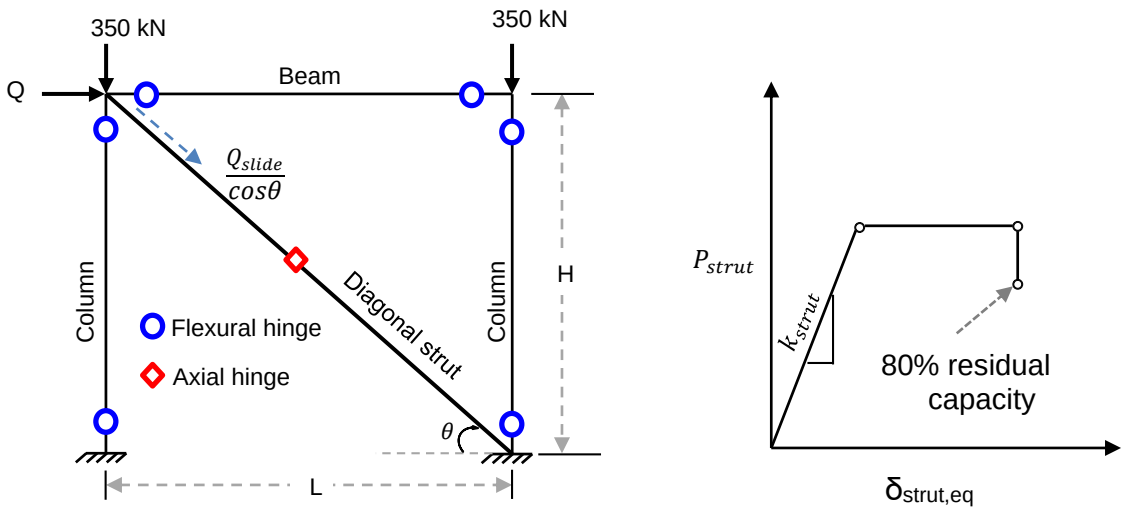

(a) *(b)*

Figure 5. Idealized (a) model of masonry infilled RC frame and (b) behaviour of strut considering sliding failure (Islam and Sen, 2023)

The initial stiffness (K_{strut}), and ultimate axial capacity (P_{strut}) of the masonry strut have been computed as per Eq. (3) - (5). The elastic and plastic axial deformation capacities of the strut have been computed as suggested by Islam and Sen (2023), which is adopted from FEMA 273 (1997). The axial hinge assignment data of the masonry strut is shown in Fig. 6(a).

$$k_{strut} = \frac{A_{strut} E_{mas}}{d_m} \tag{3}$$

$$P_{strut} = \frac{Q_{slide}}{\cos\theta} \tag{4}$$

$$Q_{slide} = \left(\frac{\tau_0}{1 - \mu \tan\theta}\right) \times L_{mas} \times t_{mas} \tag{5}$$

where, A_{strut} = area of masonry strut; E_{mas} = elastic modulus of masonry; d_m = diagonal length of masonry strut; Q_{slide} = sliding capacity of infill masonry; θ = angle of masonry strut with horizontal; τ_o = sliding strength of masonry infill (= $0.03f_{mas}$); f_{mas} = masonry prism strength; μ = friction coefficient at masonry joint, and L_{mas}/t_{mas} = length/thickness of masonry infill.

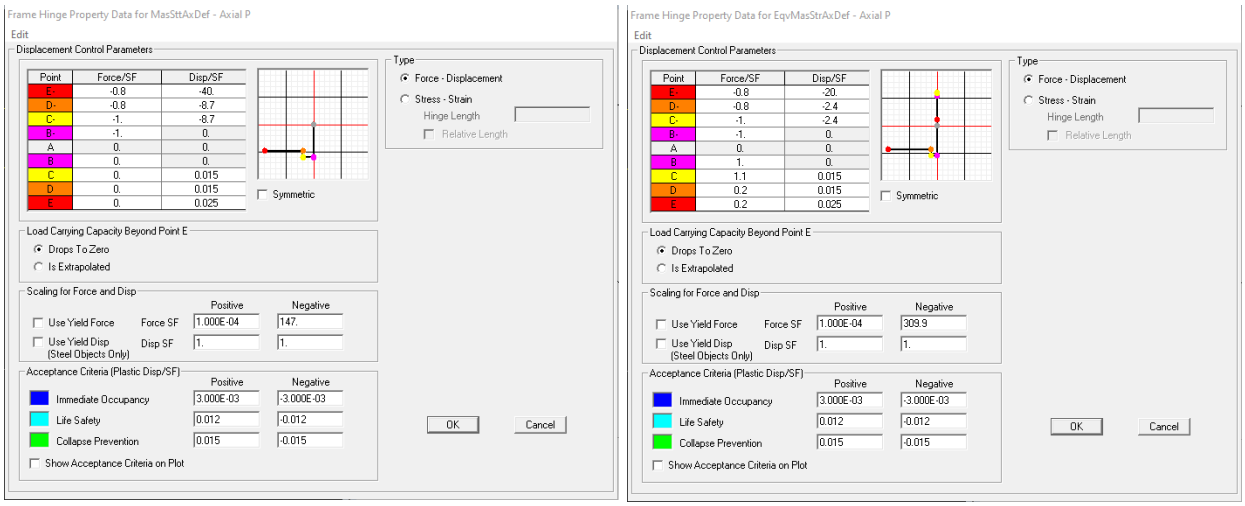

(a) *(b)*

Figure 6. Axial hinge assignment data of (a) masonry strut of masonry infilled RC frame and (b) equivalent masonry strut of FC strengthened masonry infilled RC frame

3.3 FC strengthened masonry strut

An idealized ferrocement strengthened masonry-infilled RC frame, modelled in SAP2000, is shown in Fig. 7(a). The idealized model consists of RC frame and an equivalent single masonry strut. The surrounding RC frame has been modelled in a similar way as discussed in the earlier sub-section. The equivalent single masonry strut represents the combined action of ferrocement and infill masonry; where masonry properties presented in Table 3 have been utilized. The thickness of the equivalent strut has been computed using Eq. 6 as suggested by Sen et al. (2019). The width of the strut has been computed using Eq. (6) where masonry thickness (t_{mas}) has been replaced by the term equivalent masonry thickness ($t_{eq,mas}$).

$$t_{eq,mas} = t_{mas} + n_L n_s t_{mor} \frac{E_{mor}}{E_{mas}} \tag{6}$$

where, t_{mas} = thickness of masonry; n_s = number of surfaces retrofitted with FC; n_L =number of wire mesh layers in each FC layer; t_{mor} = thickness of FC mortar layer, and E_{mas}/E_{mor} = elastic modulus of masonry and FC mortar.

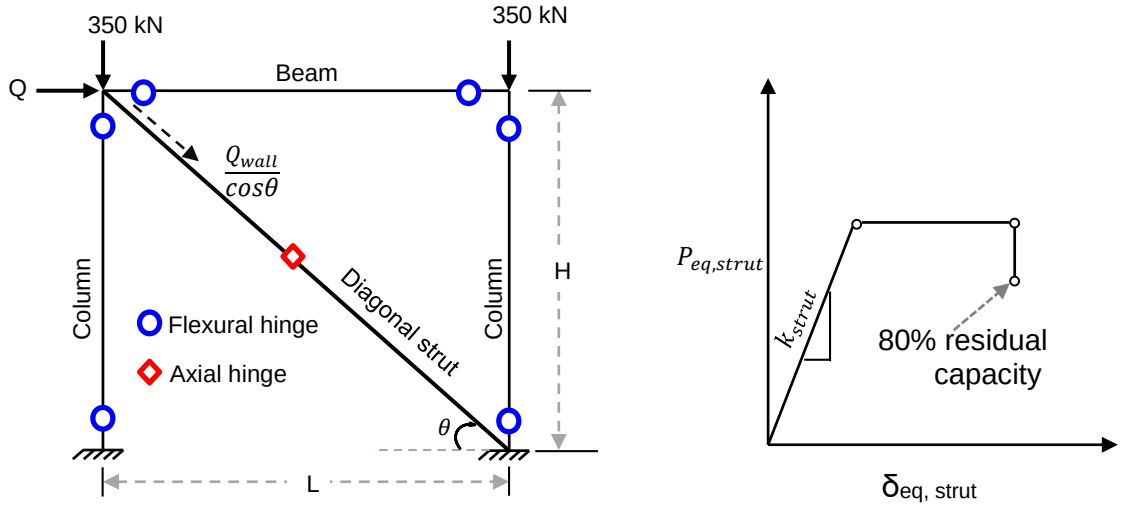

(a) *(b)*

Figure 7. Idealized (a) model of ferrocement strengthened masonry infilled RC frame and (b) behaviour of equivalent masonry strut

An axial hinge, as shown in Fig. 7(a), has been assigned at the mid-point of the equivalent diagonal strut to catch the nonlinear behaviour of the strut. The nonlinear behaviour suggested by Islam and Sen (2023) has been extended to use herein. The initial stiffness (K_{strut}) of the equivalent masonry strut has been computed as per Eq. (3); where the strut area has been computed considering the equivalent strut thickness and width of ferrocement strengthened masonry infill. Meanwhile, the axial capacity of the strut has been computed using Eq. (7) - (8) considering the diagonal cracking failure of FC strengthened masonry infill. The lateral capacity at diagonal cracking (Q_{wall}) of FC strengthened masonry infill has been adopted from Sen et al. (2020). The elastic and plastic axial deformation capacities of the strut have been computed in a similar way as discussed in an earlier subsection. The axial hinge assignment data of the masonry strut is shown in Fig. 6(b).

$$P_{eq,strut} = \frac{Q_{wall}}{Cos\theta} \tag{7}$$

$$Q_{wall} = f_{mas,cr} A_{mas} sin\theta + \alpha n_s n_L \left(\frac{h_{mas}}{s}\right) A_s f_{y,wm} \tag{8}$$

where, $f_{mas,cr}$ = cracking strength of infill masonry (= 0.05f_{mas}, f_{mas} = masonry prism strength); A_{mas} = diagonal area of infill masonry (diagonal length × masonry thickness); θ = angle of diagonal with horizontal; n_s = number of surface retrofitted with FC; n_L =number of wire mesh layer in each FC layer; h_{mas} = height of masonry infill; s = spacing of horizontal mesh reinforcements; A_s = area of horizontal wire; $f_{y,wm}$ = yield tensile strength of wire mesh, and α = empirical reduction factor (= 0.7).

4. Results and discussion

4.1 Verification of SAP2000 models

The experimental and numerical lateral load vs. story drift relationships of the reference specimens are compared as shown in Fig. 8. In the case of the bare RC frame, initial stiffness, lateral strength and drift capacities of the numerical model by SAP2000 resembled experimental observation. For the masonry-infilled RC frame model, initial stiffness and lateral strength are similar to the experimental result, however, the drift capacity ceased due to the assumed maximum displacement limit in the strut model. Meanwhile, the FC strengthened masonry infilled RC frame model in SAP2000 underestimated the initial stiffness when compared to experimental observation. This underestimation can be attributed to the fact that the surrounding RC frame was wrapped with ferrocement in experimental test which has not been considered in numerical model. Similarly, the lateral strength and drift capacities varied to a small extent. From the comparison, it is evident that the overall lateral behaviour of the reference specimens can be predicted using SAP2000 pushover analysis. The experimental and numerical lateral strength of the reference specimens are presented in Table 4.

The ratio of experimental to numerical capacities are 0.98, 1.00, and 1.07 for the bare RC frame (S1-F), masonry infilled RC frame (S3-FM), and FC laminated masonry infilled RC frame (S5-FMFC), respectively, which indicates a fair agreement with experimental results.

The hinge states at the peak resistance of the numerical models are shown in Fig. 9(a)-(c). It is evident that the plastic hinges formed at the ends of the top beam and bottom of columns in the case of all the specimens. However, in the experiment, the damage occurred initially on the beam and then concentrated on the column through load redistribution. From the hinge states at peak resistance, it is evident that the lateral capacity of the bare RC frame (S1-F) started to degrade by the collapse (○ in Fig. 9(a)) of the compressed column. On the other hand, the lateral capacity of the masonry infilled RC frame (S3-FM), and FC laminated masonry infilled RC frame (S5-FMFC) started to degrade by the collapse (○ in Fig. 9(b)-(c)) of the diagonal masonry strut.

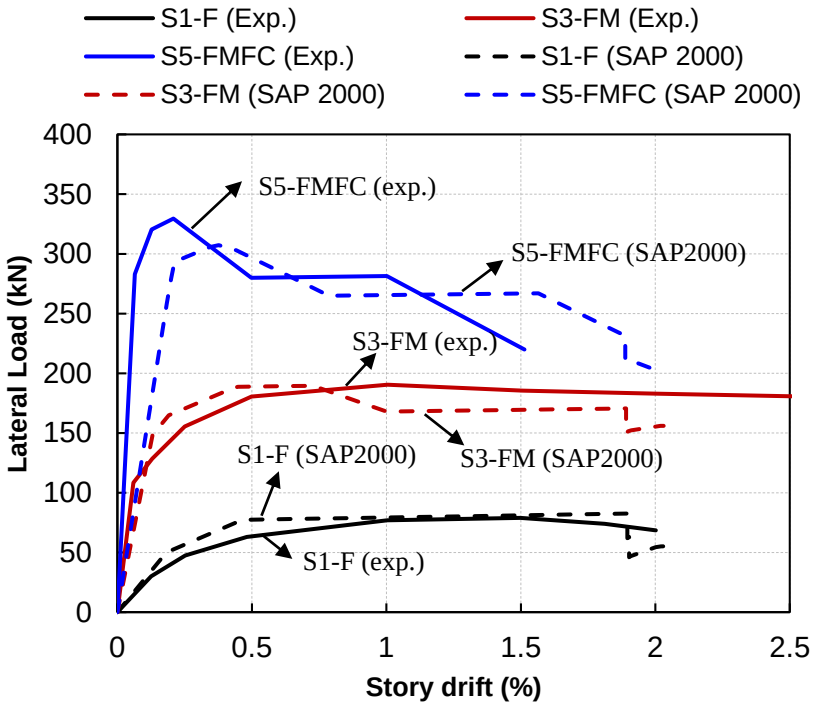

Figure 8. Comparison of lateral behaviour in the experiment and numerical model

Table 4: Comparison of experimental and numerical lateral strength

Reference specimen	**Lateral strength (kN)**		Q_{exp}/Q_{SAP}
	Experimental, Q_{exp}	**SAP2000, Q_{SAP}**	
Bare RC frame (S1-F)	79	81	0.98
Masonry infilled frame (S3-FM)	191	190	1.00
FC strengthened masonry infilled frame (S5-FMFC)	330	307	1.07

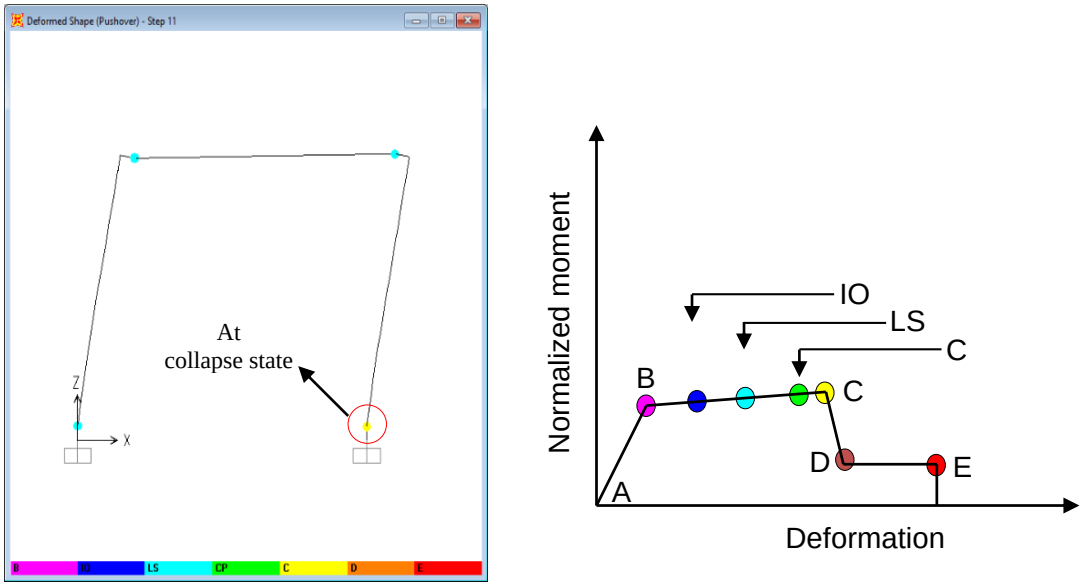

(a)

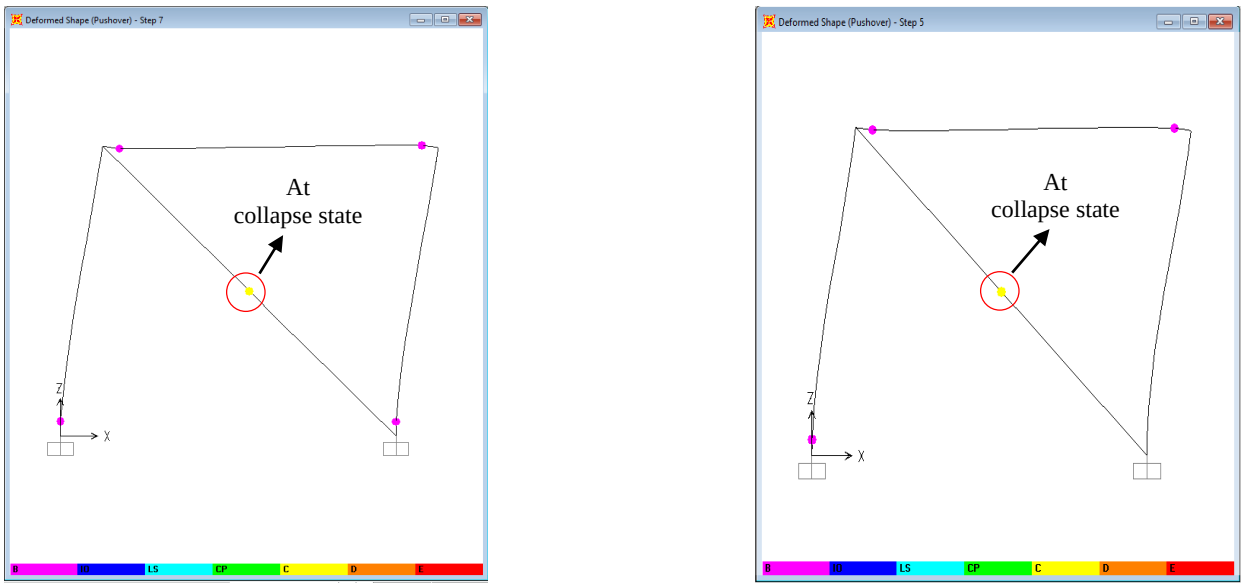

(b) *(c)*

Figure 9. Hinge formation at peak resistance of (a) S1-F, (b) S3-FM and (c) S5-FMFC

4.2 Variation of axial load on columns

In general, when lateral load is applied on a portal frame, the axial load of compression and tension side column, as shown in Fig. 10(a), increases and decreases, respectively. To investigate the performance of the adopted methodology to reflect the aforementioned phenomenon, the variation of the column axial loads, on both columns of the specimens, with the increasing story drift are shown in Fig. 10 (a)-(c). In this case, the left and right columns have been considered as tension and compression side columns, respectively since lateral load has been applied from left to right. Initially, both columns of the specimens carried the axial load of 350 kN which has been assigned as a dead load on them. After that, the axial load on the compression column and tension column gradually increased and decreased, respectively up to a certain drift level where the first hinge formed. This is followed by a sustained axial load demand until the end of the analysis.

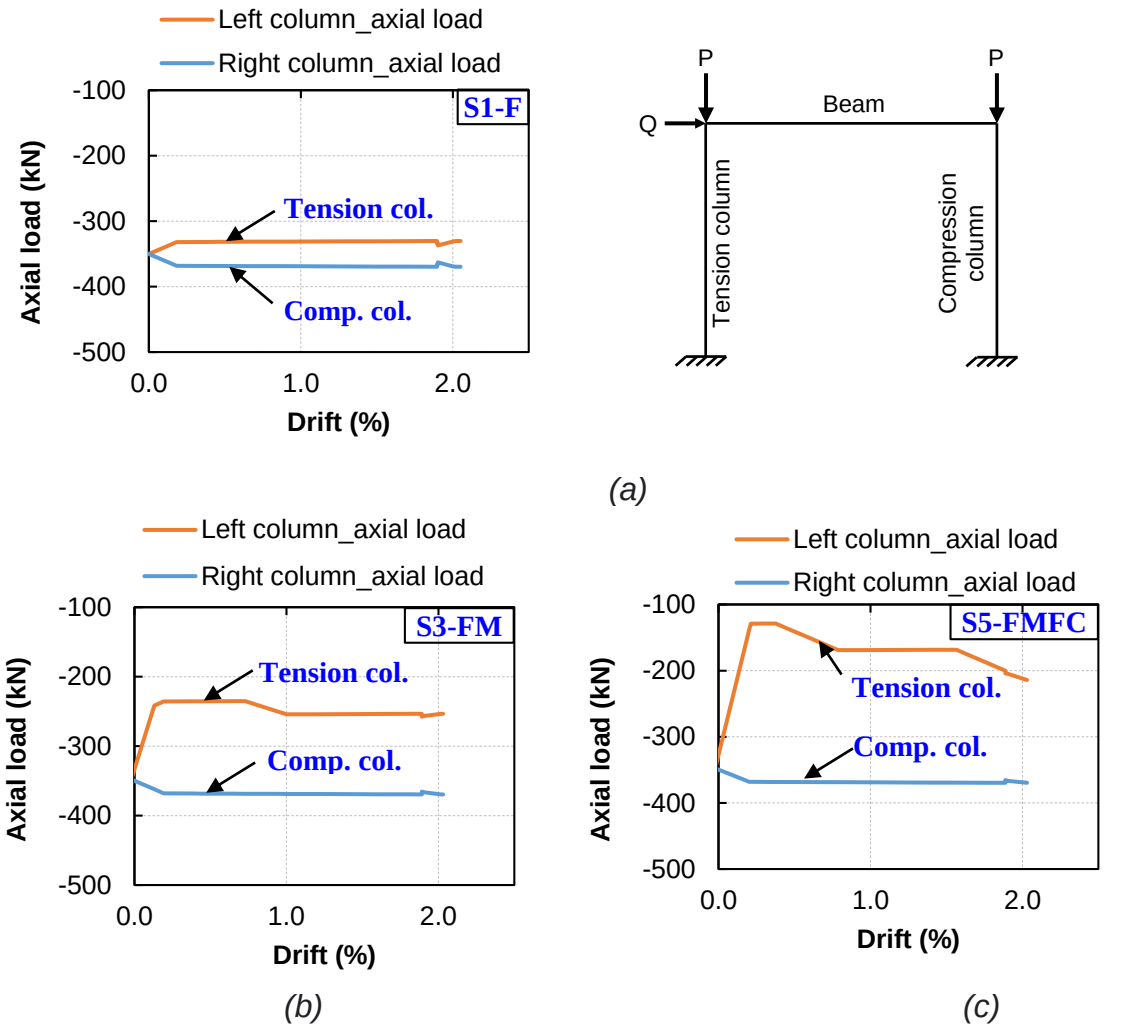

Figure 10. Variation of axial load on columns of (a) S1-F, (b) S3-FM and (c) S5-FMFC

5. Conclusion

This study focused on the simulation of lateral behaviour of bare RC frame, masonry infilled RC frame and ferrocement strengthened masonry infilled RC frame using auto lumped plastic hinges in SAP2000. Reference specimens from the authors' previous study were utilized and modelled in SAP2000 to predict the lateral behaviour of the specimens under non-linear static load. Based on the analysis result following conclusions can be drawn:

- Numerical model of bare RC frame, masonry infilled RC frame, and ferrocement strengthened masonry infilled RC frame developed using SAP2000, exhibited a fair agreement with the experimental results in terms of lateral initial stiffness, strength, and hinge formation at peak resistance with some exceptions.
- The ratio of experimental to numerical lateral capacities are 0.98, 1.00, and 1.07 for bare frame (S1-F), masonry infilled RC frame (S3-FM), and FC laminated masonry infilled RC frame (S5-FMFC), respectively.
- The developed numerical model can simulate the increase and decrease of axial load on the compression and tension side column of the RC frame, respectively; which is a general tendency of the portal frame under lateral load.
- These conclusions are based on very few specimen models; further investigation is required to apply them in the real field.

6. References

ACI Committee 549R-97 (1997). *State-of-the-Art report on ferrocement*.

Altin S., Anil Ö., Kopraman Y., Belgin Ç. (2010). Strengthening masonry infill walls with reinforced plaster, *Proceedings of the Institution of Civil Engineers: Structures and Buildings*, 163(5): 331–42.

Alwashali H., Islam M.S., Sen D., Monical J., Maeda M. (2020). Seismic capacity of RC frame buildings with masonry infill damaged by past earthquakes. *Bulletin of the New Zealand Society for Earthquake Engineering*, 53(1): 13-21, 2020. https://doi.org/10.5459/bnzsee.53.1.13-21

Amanat K.M., Alam M.M., and Alam M.S. (2007). Experimental investigation of the use of ferrocement laminates for repairing masonry in filled RC frames, *Journal of Civil Engineering (IEB)*, 35(2): 71-80.

CSI SAP2000 v.14 (2014). *Extended 3D Analysis of building System*, Computers and Structures Inc., Berkeley, California.

Demirel I.O., Yakut A., Binici B., Canbay E. (2015). An experimental investigation of infill behaviour in RC frames, *Proceeding of the 10th Pacific Conference on Earthquake Engineering*, Sydney, Australia.

FEMA 273 (1997). *NEHRP Guidelines for the Seismic Rehabilitation of Buildings, Report No. 273*, Federal Emergency Management Agency, Washington DC.

FEMA 356 (2000). *Prestandard and Commentary for the Seismic Rehabilitation of Buildings*, American Society of Civil Engineers.

Islam T., Sen D. (2023). Numerical modelling and validation of lateral behaviour of masonry-infilled RC frame focusing sliding failure of infill panel, *Asian Journal of Civil Engineering*, 24(5): 1247–1255. https://doi.org/10.1007/s42107-022-00566-1

Kaya F., Tekeli H., Anil Ö. (2018). Experimental behaviour of strengthening of masonry infilled reinforced concrete frames by adding rebar-reinforced stucco, *Structural Concrete,* 19(6):1792–1805.

Seki M., Popa V., Lozinca E., Dutu A., Papurcu A. (2018). Experimental study on retrofit technologies for RC frames with infilled brick masonry walls in developing countries, *Proceeding of the 16th European Conference on Earthquake Engineering (ECEE)*, Santiago, Chile.

Sen D (2020). Identification of failure mechanism and seismic performance evaluation of masonry infilled RC frame strengthened by ferrocement, Dissertation, Tohoku University.

Sen D., Lamsal J., Dutu A., Alwashali H., Seki M., Maeda M. (2020). Experimental study on ferro-cement retrofit for RC frame with infilled brick masonry wall, *proceeding of the 17th World Conference of Earthquake Engineering (WCEE)*, Sendai, Japan.

Sen D., Torihata Y., Alwashali H., Islam M.S., Tafheem Z., Maeda M. (2019). Investigation of the Ferro-cement laminated infilled masonry wall under cyclic lateral load, *Proceeding of the 11th Pacific Conference on Earthquake Engineering (PCEE)*, Auckland, New Zealand.

Standards Australia/Standards New Zealand (2001). *AS/NZS 4671: 2001*. Steel Reinforcing Materials.

Zarnic R., Tomazevic M. (1985). Study of the behaviour of masonry infilled reinforced concrete frames subjected to seismic loading, *Proceeding of the 7th International Conference on Brick Masonry*, Australia.